2015 IEEE 35th International Conference on Electronics and Nanotechnology (ELNANO)

Electrical Characteristics of the Carbon Nanotube Field-Effect Transistors With Extended Contacts Obtained Within *ab-initio* Based Model

Artem Fediai, Dmitry A. Ryndyk, Gianaurelio Cuniberti
Institute for Material Sciences and Max Bergmann Center of Biomaterials,
Center for Advancing Electronics Dresden,
Dresden Center for Computational Material Science,
TU Dresden, 01062 Dresden, Germany.
artem.fediai@nano.tu-dresden.de

Abstract – **In our previous work the model of the electron transport in CNTFETs with extended contacts was developed for equilibrium case using combination of the density-functional theory and equilibrium Green functions formalism. Here we extrapolate it to the case of the arbitrary biased CNTFET using simplest thinkable assumptions, which allows us to calculate drain current as a function of the gate and drain potentials. For Al and Pd electrodes we show qualitative agreement of our model with the existing experimental results both in terms of polarity of the device (*p*- or *n*-type FET) and dependence on the contact length. Most of the prediction justified by experimental data were done at *ab-initio* level for the first time.**

Keywords — carbone nanotube; Green function formalism; density functional theory; contact

I. INTRODUCTION

Carbon nanotube field effect transistors (CNTFETs) attract the interest of the scientific community as a possible substitution of the conventional MOSFETs. In a CNTFET a channel is constituted by a single or multiple carbon nanotubes, which are subjected to the field of the gate electrode and connected to the drain and source metallic electrodes. The main expectations from the CNTFET technology are attributed to the superior electron mobility ($>10^5\, cm^2/Vs$) [1] of a stand-alone CNT. As a channel of the CNTFET, however, CNT should necessarily be connected to the source and drain electrodes. This contact is the greatest obstacle in reaching the theoretical maximum of electron mobility in CNTs. As opposed to conventional electronics, metal-CNT contact resistance cannot be eliminated by the doping of the channel under the electrode as the doping of the CNT is (at least up to now) very challenging. Nevertheless, in 2003 the first CNT-FET with ohmic contacts was demonstrated. Generally, it is was not clear from the theoretical works, how the ohmic contact can be established, since it is usually not possible to reach that without the doping in conventional electronics. The possible answer was given by Nemec *et.al.* [2], [3], and in 4 years a remarkable confirmation has been obtained within experimental works of Franklin *et.al.* [4].

The main point of the works [2], [3] is the consideration of the realistic CNT-metal contacts, namely the case when the CNT is resting on the metallic electrode or is embedded into it. Within the toy model as well as the model partially based on DFT calculations it has been shown that the current can flow into the channel along the considerable length of the CNT segment embedded into the metal, and not only in the place, where the CNT channel enters an electrode. In case of embedded geometry and Pd electrode this length reaches an order of 100 nm.

Our previous work [5] is a development of the work of *Nemec et.al.* [2], [3], and allows to perform systematic treatment of the contact between the CNT any an electrode composed of any metal with direct calculation of the ballistic electron transport based on DFT Kohn-Sham Hamiltonian. By our model [5] for the first time all the relevant details of the metal-CNT contacts are taken into account, namely doping of the CNT by the metal and the strength of the electrical bonding. This, however, was done for equilibrium situation, i.e. all gate, source and drain electrode have the same potentials. This makes it possible to make some assumption about the non-equilibrium state, but not to compare simulation results with the experimental data, which are usually represented by the output and transfer characteristics, transconductance, contact resistance and their dependences on the contact length.

The aim of the current work is to use existing model of the CNT-metal contact in equilibrium state to build the simplified model of the electron transport in nonequilibrium state. The end goal is to obtain observable quantities and dependences, which in this case are static electrical characteristics. Then we compare obtained electrical characteristics with the existing experimental results to show their qualitative agreement. This could be viewed as a proof of consistency of the whole method, developed in [5].

Most of our concerns in the present work are related to the dependence of the CNTFET electrical characteristics on the contact length, and this is not accidentally. As it is mentioned in [6], the target contact length of the contact should be from 7 to 14 nm till the year 2020 to preserve the current node trend. It is thus important to be able to predict electrical properties not only for the infinite contact length, but also scaling to the

978-1-4673-6534-5/15/$31.00 ©2015 IEEE

target lengths mentioned. Till now our approach [5] is the only one, which performs correspondent calculation completely at the *ab-initio* level; we use no fitting parameter to agree with experiment.

As we do not mean to study influence of the particular geometry upon the contact, but concentrate ourselves at the main trends related to the material of the contact and its length, we accept the simplest approximation to take the biases "drain-source" and "gate-source" into account. This also makes the calculation time for each bias point reasonable, enabling calculation of the whole I-V characteristics.

II. Prerequisites to Calculate Current-Voltage Characteristics: Electron Transport in Equilibrium

In this section we summarize the results of our method developed to calculate electron transport in CNTFET in equilibrium [5]. The method is based on density functional theory as implemented in module "Quickstep" of CP2K [7]. We have used DFT as a mean to build the Hamiltonian of the atomic system closely resembling experimental geometry of the CNT-metal contact (Fig. 2). Namely, we can distinguish in this structure (1) embedded segment of the CNT with arbitrary length L_c, (2) a channel which is in fact uncovered CNT portion which has the length L_{ch}, (3) infinite electrodes comprised of the metal. To build the Hamiltonian of the system (Fig. 2) in the basis of local atomic orbitals we have simulated three finite systems, two of which were used to take the influence of the metal on embedded portion of the CNT into account; Hamiltonian of the third system served to build the Hamiltonian of the CNT itself (both free and embedded portions). This information is available in [5]. What is important in the current work, which view has an effective Hamiltonian of the system depicted in Fig. 3, a after we have decimated the metal (see Fig. 3,b). Then the system can be brought to the view (Fig. 3,c) by decimation the part, which has left after metal decimation. Two parameters (which are matrix functions) σ_ε and σ_t in Fig. 3,b is calculated in [5]. Green function of the system depicted in Fig. 3,c is the same as of the correspondent portion of the initial system. Transmission coefficient through the channel of the CNTFET of the system from Fig. 3,c is the same as for those in Fig. 3,a. Parameter σ depends on the length of the contact, so does $T(E)$. Function $T = T(E, L_c)$ is the data from equilibrium calculations which we use in this work to calculate drain current under arbitrary drain and gate potentials. Transmission coefficient as function of energy is depicted in Fig. 1 for several contact lengths. The contact length (L_c) is expressed in terms of the number of CNT unit cells (N_c).

III. Calculation of the Drain Current Within NEGF Formalism

Our intention is to construct an approximate model, which allows calculating drain-source current I_{ds} for any drain-source (φ_{ds}) and gate-source (φ_{gs}) voltages. From *ab-initio* calculation we know Hamiltonian of the nanotube and source-drain electrodes at zero voltage. We search for the simplest way to take the fields created by the electrodes under arbitrary voltages into account.

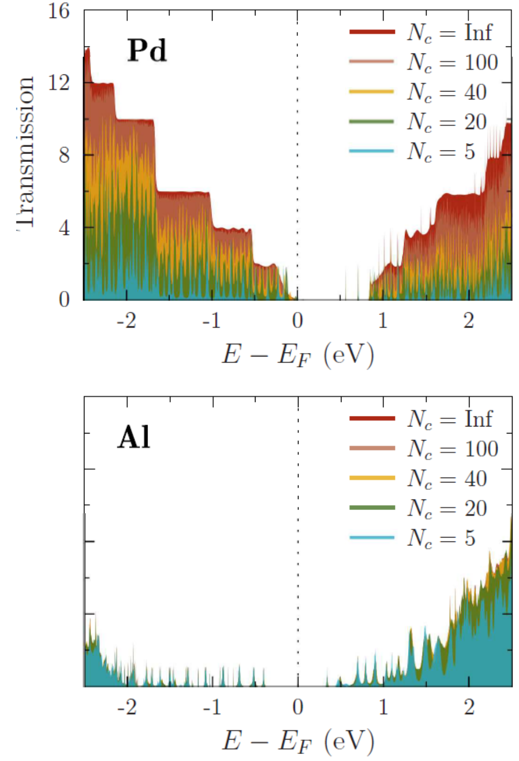

Fig. 1. Transmission coefficient as a function of energy for different contact lengths given in a number of CNT unit cells N_c for Pd and Al contacts.

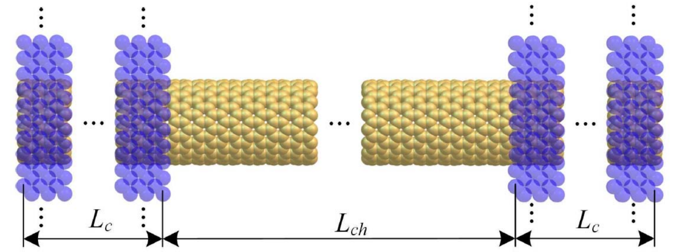

Fig. 2. Overall system of interest includes two embedded contacts and free CNT (16,0) segment in between. Transverse section of the contacts is infinite, whereas the contact length L_c is finite and arbitrary.

Within Landauer-Buttiker formalism drain current can be calculated as follows:

$$I_{ds} = \frac{2e}{h}\int_{-\infty}^{+\infty} T(E,\varphi_{gs}) \,|\, (f_s(E,\varphi_{ds}) - f_d(E,\varphi_{ds}))dE, \quad (1)$$

$$f_{s(d)}(E) = f_F(E - U_{s(d)})$$

where $f_F(E)$ is a Fermi function with $E_F = 0$.

According to our assumption, drain-source voltage φ_{ds} affects only Fermi level position in source and drain electrodes, namely: $U_s = -e\varphi_{ds}/2$ and $U_d = e\varphi_{ds}/2$. Gate-source voltage, in turns, alters transmission coefficient in non-equilibrium state T as follows: $T(E,\varphi_{gs}) = T(E - e\varphi_{gs})$ (equilibrium coefficient depends also on contact length, so does non-equilibrium one). Accepted assumptions mean that we neglect voltage drop at the channel of the tube and assume that injection properties of the contacts do not depends on bias voltage. They must capture the main trends in dependence of drain current on electrode potentials and on contact length as drain-source drops indeed mainly at the contacts; we expect, however, underestimation of the sub-threshold swing as well (reason: our assumption suppose perfect gate control), and overestimation of the drain current (non-zero gate voltage usually not only shifts transmission coefficient, but also yields its degradation).

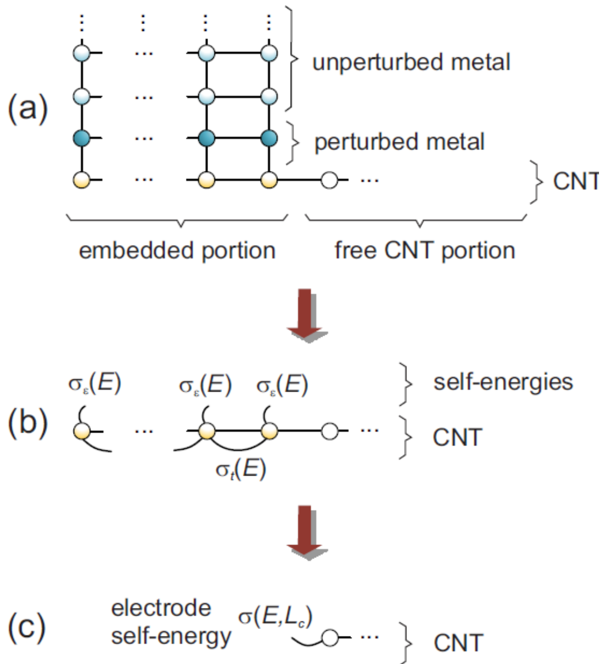

Fig. 3. Initial system, which consist of infinite metal electrode and a CNT (a) is represented by effective system which contains only carbon atoms and metal self-energies (b), which, in turns, decimates till uncovered CNT portion and self-energy affecting only the neighbouring CNT unit cell (c)

IV. RESULTS AND COMPARISON WITH EXISTING EXPERIMENTAL DATA

When compare experimental and simulated by means of our model electrical characteristics of the CNTFET, it should be noted that theoretical results are obtained having as the input quantities only coordinates of the correspondent carbon and metallic atoms; no fitting parameters were accepted neither during DFT calculation nor at NEGF stage of calculations; we have in mind also general problem in DFT with correct prediction of the band gaps. In this work we try to capture the main trends, previously *inaccessible* at *ab-initio* level, namely: preferable polarity of the CNTFET (*p*-, *n*-type or ambipolar), dependence of the contact resistance on contact length and material. Due to perfection of the simulated system geometry and accepted assumptions, our results will overestimate drain current in particular and performance of the CNTFET in general.

A. Transfer characteristics

We have simulated transfer characteristics of the CNTFET [8] with ≈9 nm channel represented by one semiconducting CNT with unknown chirality and diameter close to 1.3 nm. Experimental sample has long Pd contacts (longer than the "effective" length for Pd electrode). To predict experimental data hereafter we have used CNT with chirality (16,0), which has a diameter of approximately 1.25 nm and channel length 9.4 nm. Comparison of our calculations with the existing experiment (Fig. 4) shows that our model correctly predict polarity of the CNTFET with Pd electrodes (*p*-type FET). Pd electrodes in [8] and other experimental works yield always *p*-type FET. Overestimation of the calculated current magnitude and underestimation of the sub-threshold swing $\log(dV_{gs}/dI_{ds})$ were expected (see above); as V_{ds} increase so do discrepancies, because the basis for our calculation is stationary state, and as we go farther, our assumptions become rougher.

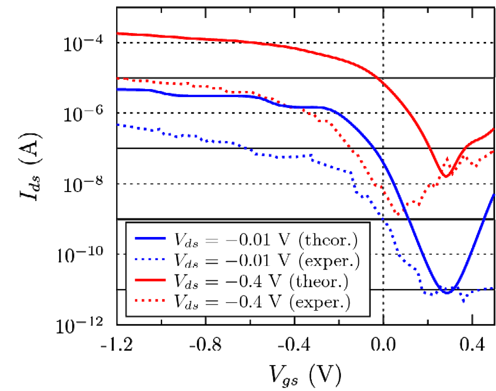

Fig. 4. Transfer characteristics of CNTFET with channel of ≈9 nm and CNT with diameter of ≈1.3 nm. Electrode material: Pd. Experimental data were adapted from [8]

B. Output characteristics depending on contact length

We have compared our calculations with the output characteristics of the set of CNT CNTFET [4] with channel length 40 nm and different contact lengths: 20, 30, 50, 70 and 100 nm. Output characteristics in both cases were measured/calculated at V_{ds} which is -1.25 V larger that the threshold voltage. Comparison of our results with the experimental data shows that we can predict current growth with the growth of the contact length. Theoretical output characteristics closely resembles Ohm's low due to very simple assumption about the electrostatics of the device. Overestimation of the theoretical value of the drain current is also expected.

Output characteristics are represented in Fig. 5. Experimental data are taken from Fig.3 of [4].

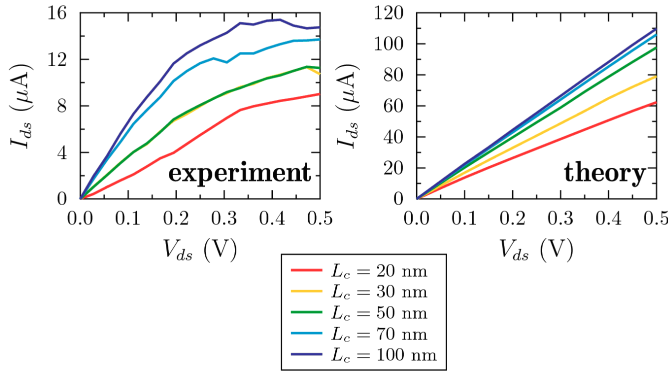

Fig. 5. Experimental and simulated characteristics of 40-nm channel CNTFET [4] with different contact length L_c. Material of the electrodes: Pd.

C. Transconductance as a function of the contact length

We have calculated the transconductance as a function of the contact length for the CNTFET [4] from the previous subsection (Fig. 6). It defines both in experiments and theory as: $g_m = dI_{ds}/dV_{gs}$ for the voltages higher than a threshold voltage. We can see that both experimental and theoretical dependences show that transconductance tends to increase till some saturated magnitude as contact length increases. Conduction magnitude difference between theoretical and experimental data is kept to be 1 order as in the case of the drain current, which is expected.

D. Influence of the Contact length on contact resistance

We have defined a contact resistance as a derivative $Rc = 1/2 \times dI_{ds}/dV_{ds}$. A work point for resistance definition was chosen at $V_{ds} = 0.5V$, $V_{gs} = -0.3V$ Fig. 7. Experimental data are taken from Fig.4 (b) of [6]. We can see that both theoretical and experimental curves behaves similarly: there is some effective contact length, after which resistance stops to decrease; as we approach zero contact length resistance grow up exponentially. Experimentally, contact resistance almost independent on drain voltage up to the work point [6] (which is itself an evidence of ohmic contact). As our assumptions are justified better at low voltages, we observe in Fig. 7 quantitative agreement with experimental dependence of $R_c(L_c)$.

E. Comparison of the CNTFETs with Pd and Al contacts

In our previous work [5] we have discovered that embedded into metallic electrode tube portion in case of Pd electrode is being metal-doped whereas in case of Al is fully metallized (no band gap). Our calculations (Fig. 8) show, which consequences it has from the point of view of the contact resistance, which has been calculated in the same manner as described above. Aluminium contacts are not sensitive to the length of the contact up to contact length close to 1 nm in contrast to Pd contacts. As expected, Al contact has several orders higher resistance than Pd one, as high reflection take place between drastically modified portion of the tube and the uncovered tube portion.

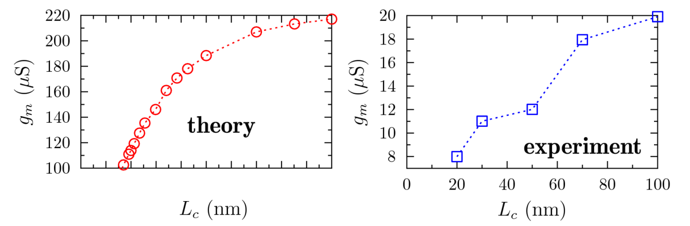

Fig. 6. Transconductance of the CNTFET [4] with Pd electrode (theory vs. experiment).

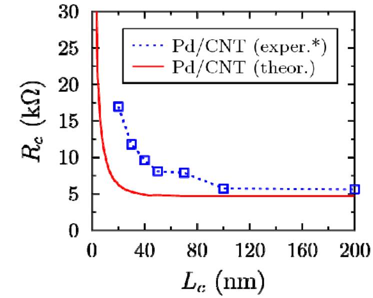

Fig. 7. Dependence of the contact resistance on contact length for Pd contact. Experimental data are taken from [6].

In Fig. 9 we finally present transfer characteristics for both Pd and Al contacts. The main difference between CNTFET with Pd contacts and that with Al contacts is a polarity of the device: Pd contacts yield *p*-type FET; Al contacts yield ambipolar FET with the signs of *n*-type polarity. In experimental set-ups Al-contacted CNTFET usually show more prominent *n*-type behaviour [9], although, there is no results on Al contacts to compare directly with our model system.

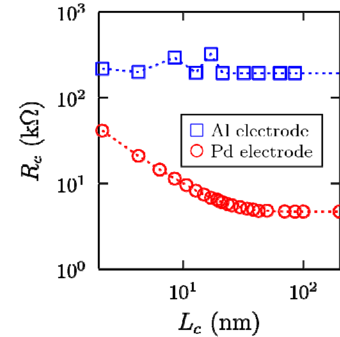

Fig. 8. Dependence of the contact resistance on contact length: comparison between Pd and Al contacts

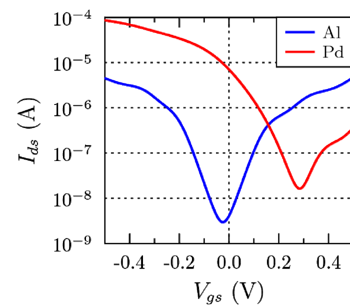

Fig. 9. Calculated transfer characteristics for Al- and Pd-contacted CNTFETs

CONCLUSION

In conclusion, we have developed DFT-NEGF based model to predict static electrical characteristics of the CNTFET with Al and Pd contacts. The model is shown to be able to predict correct polarity of the CNTFET with Pd and Al electrodes. This follows from the comparison of with experimental transfer characteristics. Our model predict experimental trends in the dependences of transconductance and contact resistance for Pd-contacted FET. Namely, contact resistance in both our simulation and experimental data drops as contact length increase up to some effective length. We have shown also that Al-contacted CNTFETs are not sensible to contact length in contrast to Pd-contacted ones. This finding should be yet confirmed experimentally. Finally, we demonstrate higher contact resistance for Al contact compared to Pd contacts, which can be explained by stronger interaction with Carbon; preferable polarity of the Pd- and Al-contacted CNTFETs is opposite which is in qualitative agreement with existing experiments.

ACKNOWLEDGMENT

We acknowledge the Center for Information Services and High Performance Computing (ZIH) at TU Dresden for computational resources. This work is partly supported by the German Research Foundation (DFG) within the Cluster of Excellence "Center for Advancing Electronics Dresden".

REFERENCES

[1] T. Drkop, S. A. Getty, E. Cobas, and M. S. Fuhrer, “Extraordinary mobility in semiconducting carbon nanotubes,” Nano Letters, vol. 4, no. 1, pp. 35–39, 2004. [Online]. Available: http://dx.doi.org/10.1021/nl034841q

[2] N. Nemec, D. Tomanek, and G. Cuniberti, “Contact dependence of carrier injection in carbon nanotubes: An ab initio study,” Phys. Rev. Lett., vol. 96, p. 076802, Feb 2006. [Online]. Available: http://link.aps.org/doi/10.1103/PhysRevLett.96.076802

[3] N. Nemec, D. Tom´anek, and G. Cuniberti, “Modeling extended contacts for nanotube and graphene devices,” Phys. Rev. B, vol. 77, p. 125420, Mar 2008. [Online]. Available: http://link.aps.org/doi/10.1103/PhysRevB.77.125420

[4] A. D. Franklin and Z. Chen, “Length scaling of carbon nanotube transistors,” Nat Nano, vol. 5, no. 12, pp. 858–862, Dec. 2010. [Online]. Available: http://dx.doi.org/10.1038/nnano.2010.220

[5] A. Fediai, D. Ryndyk, and G. Cuniberti, “Electron transport in extended cnt-metal contacts: rigorous ab-initio based green function method,” (submitted to Phys. Rev. B).

[6] A. D. Franklin, D. B. Farmer, and W. Haensch, “Defining and overcoming the contact resistance challenge in scaled carbon nanotube transistors,” ACS Nano, vol. 8, no. 7, pp. 7333–7339, 2014, pMID: 24999536. [Online]. Available: http://dx.doi.org/10.1021/nn5024363

[7] J. VandeVondele, M. Krack, F. Mohamed, M. Parrinello, T. Chassaing, and J. Hutter, “Quickstep: Fast and accurate density functional calculations using a mixed gaussian and plane waves approach,” Computer Physics Communications, vol. 167, no. 2, pp. 103 – 128, 2005. [Online]. Available: http://www.sciencedirect.com/science/article/pii/S0010465505000615

[8] A. D. Franklin, M. Luisier, S.-J. Han, G. Tulevski, C. M. Breslin, L. Gignac, M. S. Lundstrom, and W. Haensch, “Sub-10 nm carbon nanotube transistor,” Nano Letters, vol. 12, no. 2, pp. 758–762, 2012, pMID: 22260387. [Online]. Available: http://dx.doi.org//10.1021/nl203701g

[9] A. Javey, Q. Wang, W. Kim, and H. Dai, “Advancements in complementary carbon nanotube field-effect transistors,” in Electron Devices Meeting, 2003. IEDM ’03 Technical Digest. IEEE International, Dec 2003, pp. 31.2.1–31.2.4.